

Simple Detection Schemes for the Alamouti Code Assisted V-BLAST (ACAV) System

David Wee-Gin Lim

*Department of Electrical and Electronic Engineering
The University of Nottingham Malaysia Campus
43500 Semenyih, Selangor, Malaysia.
Email: lim.wee-gin@nottingham.edu.my*

Abstract—The Alamouti Code Assisted V-BLAST (ACAV) is a promising hybrid MIMO transmission scheme that is adopted by IEEE 802.11n-2009 (WiFi) recently. It combines spatial multiplexing (SM) and Alamouti space-time block codes (STBC) so that if the Alamouti symbols were detected first, which are generally more reliable due to STBC, subsequent interference cancelation (IC) stages will suffer less from error propagation. The optimal IC detector for the ACAV can be undesirably complex but we found a procedure to reduce the complexity and processing time without compromising its optimality. We further developed a simpler suboptimal detector that is suitable for rapidly varying channels. Simulation results show both ACAV detectors can outperform the detectors of pure SM scheme of the same data rate.

Keywords-Hybrid transmission scheme; ACAV; STBC-VBLAST; MIMO detector; MIMO detection scheme

I. INTRODUCTION

At the turn of the millennium, the multiple-input and multiple-output (MIMO) system has emerged as a promising technology for high data-rate broadband wireless communications. Traditional MIMO schemes either achieve diversity gain to increase the link reliability against fading, e.g., Alamouti space-time block code (STBC) [1], [2], or achieve spatial multiplexing (SM) gain to increase spectral efficiency and data throughput, assuming there is sufficient signal scattering and antenna spacing, e.g., Vertical Bell Labs Layered Space-Time (V-BLAST) [3]. More recently, hybrid MIMO transmission schemes (HMTS) [4] have been proposed to achieve a finer trade off between pure diversity gain and pure SM gain so that parts of the data are space-time coded across some antennas and others are spatially multiplexed. A number of the HMTS have been included in the recent WiFi (IEEE 802.11n-2009 [5]) and WiMAX (IEEE 802.16-2009 [6]) standards.

Among the HMTS that are described in [4], this paper addresses a special family of HMTS called the Alamouti-Code-Assisted-VBLAST (ACAV) – a term coined by Zhang *et al* [7]. Two of its M_t transmit antennas are assigned to transmit 2×2 Alamouti STBC data streams while the remaining $M_t - 2$ antennas are used to transmit independent V-BLAST SM data streams. The ACAV is equivalent to HMTS G2+1 for 3 antenna and G2+1+1 for 4 antenna in

Table I
ANTENNA MAPPING FOR THE SPACE/TIME CODE-RATE 3 ACAV USING FOUR TRANSMIT ANTENNAS [5]

Rate-3 (6 symbols in 2 symbol periods)				
Time Slot	Ant 1	Ant 2	Ant 3	Ant 4
1	$a_1(k)$	$a_2(k)$	$a_3(k)$	$a_4(k)$
2	$-a_2^*(k)$	$a_1^*(k)$	$a_5(k)$	$a_6(k)$

Table II
ANTENNA MAPPING FOR SPACE/TIME CODE-RATE 1, 2 AND 4 TRANSMIT SCHEMES OF IEEE 802.16E-2005 [8]

Rate-1				
Time Slot	Ant 1	Ant 2	Ant 3	Ant 4
1	$a_1(k)$	$a_2(k)$	-	-
2	$-a_2^*(k)$	$a_1^*(k)$	-	-
3	-	-	$a_3(k)$	$a_4(k)$
4	-	-	$-a_4^*(k)$	$a_3^*(k)$

Rate-2				
Time Slot	Ant 1	Ant 2	Ant 3	Ant 4
1	$a_1(k)$	$a_2(k)$	$a_3(k)$	$a_4(k)$
2	$-a_2^*(k)$	$a_1^*(k)$	$-a_4^*(k)$	$a_3^*(k)$
3	$a_5(k)$	$a_6(k)$	$a_7(k)$	$a_8(k)$
4	$-a_6^*(k)$	$a_5^*(k)$	$-a_8^*(k)$	$a_7^*(k)$

Rate-4				
Time Slot	Ant 1	Ant 2	Ant 3	Ant 4
1	$a_1(k)$	$a_2(k)$	$a_3(k)$	$a_4(k)$

[4]. The 4 antenna ACAV delivers 3 spatial substreams [5] since 6 data symbols are transmitted over 2 symbol periods (see Table I). Alternatively, the ACAV is said to achieve a space/time code-rate of 3 [8]. In fact the older IEEE 802.16e-2005 standard [8] only outlined HMTS of rates-1, -2 and -4 for a 4×4 MIMO system (see Table II), so the rate-3 ACAV bridges the gap in space/time code-rate.

The IEEE standards do not define the type of data detectors to be used for each HMTS. In the literature, two types of ACAV detectors have been reported and they can be loosely categorized as single stage and dual stage detectors. The single stage detector includes the likes of the linear detector (Lin) and the ordered-successive-interference-cancelation (OSIC)¹ non-linear detector, e.g., [9]. These detectors operate on an *inflated* channel matrix of dimension $2M_r \times 2(M_t - 1)$, rather than the original $M_r \times M_t$ matrix,

¹Even though the OSIC involves several sequential stages or iterations, we still consider the procedure as a single stage.

in order to effectively exploit the diversity gain of the STBC which spans two symbol periods. This increased matrix size imposes approximately exponential burden on detector complexity for every extra matrix column. The inflated channel matrix can be avoided to reduce complexity but not without sacrificing the bit-error-rate (BER) performance. This can be done through the use of a dual stage detector which first detects the Alamouti symbols (henceforth called A-symbols, and the V-BLAST symbols as V-symbols) using a sort of MIMO spatial filter of dimension $M_t \times M_r$, and then cancel its interference, before detecting the remaining V-symbols in the second stage, for e.g., [4].

In Section II, the system model is outlined and the architecture of the ACAV briefly reviewed. Section III outlines our proposed reduced complexity single-stage ACAV detector. Section IV describes another reduced complexity dual-stage detector. Section V presents complexity and simulation results. The paper is finally concluded in Section VI.

II. SYSTEM MODEL & THE ACAV ARCHITECTURE

In this paper, we consider the 3×3 and 4×4 MIMO systems in accordance to IEEE 802.16e-2005 [8] and IEEE 802.11n-2009 [5]. The antenna mappings for a block of 6 ACAV symbols are given in Table I. The source symbols are drawn independently from the same alphabet set and grouped into “space-time blocks” of $2(M_t - 1)$ symbols. The first two symbols $a_1(k)$ and $a_2(k)$ are Alamouti encoded and the rest are spatially multiplexed (V-BLAST). The transmission patterns of rate-1, -2 and -4 schemes of IEEE 802.16e-2005 are provided in Table II for comparison.

At the channel output, the received vector is governed by the following channel input-output relationship

$$\mathbf{r}(k) = \mathbf{H}\mathbf{a}(k) + \mathbf{n}(k) \quad (1)$$

where k denotes a space-time block sample occupying two symbol periods, $\mathbf{r}(k) \triangleq [\mathbf{r}_1(k), \mathbf{r}_2(k)] \in \mathbb{C}^{M_r \times 2}$, $\mathbf{H} \triangleq [\mathbf{H}_A, \mathbf{H}_V] = [\mathbf{h}_1, \mathbf{h}_2, \dots, \mathbf{h}_{M_t}] \in \mathbb{C}^{M_r \times M_t}$ is the Rayleigh flat fading channel (N.B.: $\mathbf{H}_A = [\mathbf{h}_1, \mathbf{h}_2] \in \mathbb{C}^{M_r \times 2}$ denotes the Alamouti subchannels, $\mathbf{H}_V = [\mathbf{h}_3, \dots, \mathbf{h}_{M_t}] \in \mathbb{C}^{M_r \times (M_t - 2)}$ denotes the V-BLAST subchannels), $\mathbf{a}(k) \in \mathbb{C}^{M_t \times 2}$ denotes the source signals, whose energy is σ_a^2 , in the manner shown in Table I and $\mathbf{n}(k) \in \mathbb{C}^{M_r \times 2}$ is the additive white Gaussian noise (AWGN) matrix with a complex variance of σ_n^2 . One way of data detection is to process the received vector $\mathbf{r}(k)$ using a MIMO spatial filter to extract the A-symbols because they are usually more reliable, and subsequently perform interference cancelation to detect the remaining V-symbols [4]. We refer to this method as the dual-stage detector which we pursue in Section IV. To achieve better BER suppression, we should consider the inflated channel matrix, $\tilde{\mathbf{H}}$, defined below, which takes into account all $2(M_t - 1)$ symbols so that the transmit diversity can be more effectively exploited [9], so that detection is

carried out in a single stage:

$$\tilde{\mathbf{r}}(k) = \tilde{\mathbf{H}}\tilde{\mathbf{a}}(k) + \tilde{\mathbf{n}}(k) \Rightarrow \begin{bmatrix} \mathbf{r}_1(k) \\ \mathbf{r}_2^*(k) \end{bmatrix} = \begin{bmatrix} \mathbf{H}_A & \mathbf{H}_V & \mathbf{0}_2 \\ \mathcal{A}(\mathbf{H}_A) & \mathbf{0}_2 & \mathbf{H}_V^* \end{bmatrix} \tilde{\mathbf{a}}(k) + \begin{bmatrix} \mathbf{n}_1(k) \\ \mathbf{n}_2^*(k) \end{bmatrix} \quad (2)$$

where the “Alamouti” operator $\mathcal{A}([\mathbf{h}_1, \mathbf{h}_2]) \triangleq [\mathbf{h}_2^*, -\mathbf{h}_1^*]$, $\mathbf{0}_2$ is a zero matrix of dimension $M_r \times 2$ and $\tilde{\mathbf{a}}(k) = [a_1(k), a_2(k), a_3(k), a_4(k), a_5^*(k), a_6^*(k)]^T$. The special structure inherent in $\tilde{\mathbf{H}}$ is the motivation behind the design of the low-complexity pair-wise OSIC detector in the following Section III.

III. REDUCED COMPLEXITY SINGLE STAGE DETECTOR: PAIR-WISE OSIC (PWO)

In the following we propose a modified OSIC scheme which decodes twice as fast, uses less computations, but attains identical BER performance as the original OSIC for ACAV [3].

A. Data Detection in Pairs

Let’s consider only the zero-forcing (ZF) detector (extension to the MMSE detector is straight forward). Let $\tilde{\mathbf{G}}$ denote the Moore-Penrose pseudoinverse of $\tilde{\mathbf{H}}$. Subject to the condition that the matrix $\tilde{\mathbf{G}}$ must have an even number of rows, the pseudoinverse has this specific form:

$$\tilde{\mathbf{G}} = \tilde{\mathbf{H}}^\dagger = \begin{bmatrix} \mathbf{G}_A & \mathcal{A}(\mathbf{G}_A) \\ \mathbf{G}_{V1} & -\mathbf{G}_{V2}^* \\ \mathbf{G}_{V2} & \mathbf{G}_{V1}^* \end{bmatrix} \quad (3)$$

where $\mathbf{G}_A, \mathbf{G}_{V1}, \mathbf{G}_{V2}$ are all $2 \times M_r$ matrices. Expanding (3), it can be shown that the row-norms of certain subchannels $\tilde{\mathbf{G}}$ are identical, since all elements of one row have counterparts of same magnitude in one other row. They are the 1st and 2nd row, 3rd and 5th row, and finally the 4th and 6th row. Since the row-norms are identical for the two subchannels within the pair, that means both symbols that belong to the equal-norm subchannels can be detected simultaneously *without any loss in optimality* at all.

B. Optimal Sorting with Detection Speed Doubled

According to [3], the optimal sorting is based on selecting first the subchannel which has the minimum norm. The A-symbols are most robust to noise and therefore with high probability, their corresponding subchannels in $\tilde{\mathbf{G}}$ have minimum norms. This is because their corresponding columns in $\tilde{\mathbf{H}}$ (c.f. Eq. (2)) consist of only non-zero elements, i.e., $[\mathbf{H}_A \ \mathcal{A}(\mathbf{H}_A)]^T$, while the columns of the other V-subchannels are occupied half of the time by 0, i.e., $([\mathbf{H}_V \ \mathbf{0}_2]^T$ and $[\mathbf{0}_2 \ \mathbf{H}_V^*]^T)$. The robustness of the A-symbols is a consequence of STBC of $a_1(k)$ and $a_2(k)$. However, optimality is not guaranteed if the A-symbols were detected and canceled first because one of the V-subchannels may have a higher SNR than the A-subchannel for a

Table III
PAIR-WISE ORDERED SEQUENTIAL DETECTION

Let the j -th row of $\tilde{\mathbf{G}}$ be denoted as $(\tilde{\mathbf{G}})_j$.
 Let $k_i(1)$ and $k_i(2)$ denote the indices of the 1st and 2nd symbols,
 respectively, of the symbol-pair with equal SNR, at the i -th iteration/
 OSIC stage.
 $\mathbb{Q}(\cdot)$ is the nearest neighbour hard quantization operator.
 $\tilde{\mathbf{H}}^{(i)}$ is the deflated channel matrix of $\tilde{\mathbf{H}}$ at the i -th iteration.

Initialization:
 $i = 1$
 $\tilde{\mathbf{r}}_1(k) = \tilde{\mathbf{r}}(k)$
 $\tilde{\mathbf{G}}_1 = (\tilde{\mathbf{H}})^\dagger$

Recursion:

$$\mathbf{w}_i^{zf} = \begin{bmatrix} (\tilde{\mathbf{G}}_i)_{k_i(1)} \\ (\tilde{\mathbf{G}}_i)_{k_i(2)} \end{bmatrix}$$

$$\begin{bmatrix} \tilde{z}_{k_i(1)}(k) \\ \tilde{z}_{k_i(2)}(k) \end{bmatrix} = \mathbf{w}_i^{zf} \tilde{\mathbf{r}}_i(k)$$

$$\begin{bmatrix} \hat{a}_{k_i(1)}(k) \\ \hat{a}_{k_i(2)}(k) \end{bmatrix} = \begin{bmatrix} \mathbb{Q}(\tilde{z}_{k_i(1)}(k)) \\ \mathbb{Q}(\tilde{z}_{k_i(2)}(k)) \end{bmatrix}$$

$$\tilde{\mathbf{r}}_{i+1}(k) = \tilde{\mathbf{r}}_i(k) - [\mathbf{h}_{k_i(1)}, \mathbf{h}_{k_i(2)}] \begin{bmatrix} \hat{a}_{k_i(1)}(k) \\ \hat{a}_{k_i(2)}(k) \end{bmatrix}$$

$$\tilde{\mathbf{G}}_{i+1} = (\tilde{\mathbf{H}}^{(i)})^\dagger$$

$$i = i + 1$$

particular channel realization. Thus, to retain optimality, all the row norms of $\tilde{\mathbf{G}}$ are still calculated just in case the A-subchannel is not the strongest. Subsequently the symbols, be it A- or V-, are detected and canceled according to the OSIC algorithm of [3]. This interference cancellation (IC) process is performed on the symbol-pair simultaneously so the number of sequential IC stages is halved. Table III summarizes this pair-wise OSIC (PWO) algorithm.

IV. REDUCED COMPLEXITY DUAL STAGE DETECTOR: GROUP-LINEAR (GL) AND GROUP-OSIC (GO)

Both the PWO algorithm in Section III and the OSIC of [9] deal with an inflated channel matrix $\tilde{\mathbf{H}}$. Trading off BER performance slightly to enjoy lower pre-processing burden (e.g., the pseudo-inverse operation), a dual stage detector may be employed to detect the ACAV symbols by using only the $M_r \times M_t$ channel matrix. In the first stage, the A-symbols are detected using a group receiver [10], followed by interference cancellation (IC) and the detection of the V-symbols using a linear or OSIC detector. Thus we name our dual-stage detectors as the Group-Linear (GL) and the Group-OSIC (GO) detectors. They are especially beneficial in rapidly time-varying channels when the pre-processing cost is significant as compared to the cost of payload processing (i.e., computation required to process every symbol of frame).

A. Stage-1: Zero-forcing (ZF) Group Receiver

The ZF group receiver partitions the original channel matrix into four quadrants as follows [11]:

$$\mathbf{H} \triangleq \begin{bmatrix} \mathbf{A} & \mathbf{B} \\ \mathbf{C} & \mathbf{D} \end{bmatrix} \quad (4)$$

where $\mathbf{A} \in \mathbb{C}^{2 \times 2}$, $\mathbf{B} \in \mathbb{C}^{2 \times (M_t - 2)}$, $\mathbf{C} \in \mathbb{C}^{(M_r - 2) \times 2}$, and $\mathbf{D} \in \mathbb{C}^{(M_r - 2) \times (M_t - 2)}$. \mathbf{A} always carries the top left entries of \mathbf{H} of dimension 2×2 , i.e.,

$$\mathbf{A} \triangleq \begin{bmatrix} h_{11} & h_{12} \\ h_{21} & h_{22} \end{bmatrix}, \quad (5)$$

where h_{ij} is the element in the i -th row and j -th column of \mathbf{H} . Subsequently, ZF group equalization is performed on $\mathbf{r}(k)$. The ZF group equalizer takes the following form:

$$\mathbf{W}^{zf} = \begin{bmatrix} \mathbf{B}^{-1} & -\mathbf{D}^{-1} \\ \mathbf{A}^{-1} & -\mathbf{C}^{-1} \end{bmatrix} \quad (6)$$

so that the combined channel-group-equalizer response,

$$\mathbf{W}^{zf} \mathbf{H} = \begin{bmatrix} \mathbf{B}^{-1} \mathbf{A} - \mathbf{D}^{-1} \mathbf{C} & \mathbf{0}_{2r} \\ \mathbf{0}_{c2} & \mathbf{A}^{-1} \mathbf{B} - \mathbf{C}^{-1} \mathbf{D} \end{bmatrix} \quad (7)$$

is a diagonal matrix that isolates the two A-substreams from the V-substreams. $\mathbf{0}_{2r}$ and $\mathbf{0}_{c2}$ are zero matrices of dimensions $2 \times (M_t - 2)$ and $(M_t - 2) \times 2$, respectively. As a result, the virtual channel of the A-substreams due to the ZF group receiver is

$$\tilde{\mathbf{H}}_A \triangleq \mathbf{B}^{-1} \mathbf{A} - \mathbf{D}^{-1} \mathbf{C} \quad (8)$$

where $\tilde{\mathbf{H}}_A \in \mathbb{C}^{(M_t - 2) \times 2}$. The received signal after the group receiver can be expressed as

$$\mathbf{s}(k) \triangleq \begin{bmatrix} \mathbf{s}_A(k) \\ \mathbf{s}_V(k) \end{bmatrix} = \mathbf{W}^{zf} \mathbf{r}(k) = \mathbf{W}^{zf} \mathbf{H} \mathbf{a}(k) + \tilde{\mathbf{n}}(k), \quad (9)$$

where $\mathbf{s}_A(k) \in \mathbb{C}^{2 \times 2}$, $\mathbf{s}_V(k) \in \mathbb{C}^{(M_t - 2) \times 2}$ and $\tilde{\mathbf{n}}(k) \in \mathbb{C}^{M_t \times 2}$ is the filtered noise matrix. We have deliberately divided $\mathbf{s}(k)$ into two matrices because we only want to retrieve $\mathbf{s}_A(k)$ that corresponds to the Alamouti stream, i.e.,

$$\mathbf{s}_A(k) = [\mathbf{B}^{-1}, -\mathbf{D}^{-1}] \mathbf{r}(k). \quad (10)$$

Using $\mathbf{s}_A(k)$ from (10), the optimal maximum likelihood soft decisions of the A-symbols are obtained as follows

$$\begin{bmatrix} \tilde{z}_1(k) \\ \tilde{z}_2^*(k) \end{bmatrix} = \left[\|\tilde{\mathbf{H}}_A\|_F^2 \right]^{-1} (\tilde{\mathbf{H}}_{A2})^H \tilde{\mathbf{s}}(k) \quad (11)$$

where $\|\cdot\|_F$ denotes the Frobenius norm, $(\cdot)^H$ denotes the Hermitian operation (complex conjugate transpose),

$$\tilde{\mathbf{H}}_{A2} \triangleq \begin{bmatrix} \tilde{\mathbf{H}}_A \\ \mathcal{A}(\tilde{\mathbf{H}}_A) \end{bmatrix} \quad (12)$$

where $\mathcal{A}(\mathbf{x}) \triangleq \mathcal{A} \left(\begin{bmatrix} a & b \\ c & d \end{bmatrix} \right) = \begin{bmatrix} b^* & -a^* \\ d^* & -c^* \end{bmatrix}$, and $\tilde{\mathbf{s}}(k) \triangleq [s_{11}(k), s_{12}^*(k)]^T$ if $M_t = M_r = 3$ where $\mathbf{s}_A(k) = [s_{11}(k), s_{12}(k)]$, or $\tilde{\mathbf{s}}(k) \triangleq [s_{11}(k), s_{21}(k), s_{12}^*(k), s_{22}^*(k)]^T$

if $M_t = M_r = 4$ where $\mathbf{s}_A(k) \equiv \begin{bmatrix} s_{11}(k) & s_{12}(k) \\ s_{21}(k) & s_{22}(k) \end{bmatrix}$. Subsequently, a nearest neighbour quantizer $\mathbb{Q}(\cdot)$ is used to estimate the A-symbols: $[\hat{a}_1(k), \hat{a}_2(k)]^T = [\mathbb{Q}(\hat{z}_1(k)), \mathbb{Q}(\hat{z}_2(k))]^T$.

After the A-symbols have been detected, they will be canceled from the received signals, $\mathbf{r}(k)$, as follows:

$$\mathbf{t}(k) \triangleq [\mathbf{t}_1(k) \ \mathbf{t}_2(k)] = \mathbf{r}(k) - [\mathbf{h}_1 \ \mathbf{h}_2] \begin{bmatrix} \hat{a}_1(k) & -\hat{a}_2^*(k) \\ \hat{a}_2(k) & \hat{a}_1^*(k) \end{bmatrix}. \quad (13)$$

$\mathbf{t}_1(k) \in \mathbb{C}^{M_t \times 1}$ and $\mathbf{t}_2(k) \in \mathbb{C}^{M_t \times 1}$ are the column vectors that correspond to the V-symbols of the first and second time slot in block k , respectively. If the decisions $\hat{a}_1(k)$ and $\hat{a}_2(k)$ are correct, then $\mathbf{t}(k)$ will enjoy a large diversity gain since the the V-symbols are effectively being transmitted from $M_t - 2$ antennas but are received by two more receive antennas! Moreover, the signals from the first time slot of space-time block k are now independent of those signals from the second time slot, so the detection of V-symbols is carried out with a much smaller deflated channel matrix *one time slot at a time*.

B. Stage-2: Linear detection or OSIC

In stage 2, we can use either the linear or the OSIC algorithm. The effective channel affecting the remaining V-symbols is $\mathbf{H}_V = [\mathbf{h}_3]$ for the 3×3 ACAV, or $\mathbf{H}_V = [\mathbf{h}_3 \ \mathbf{h}_4]$ for the 4×4 ACAV. Both the linear detection algorithm and the first step of the OSIC algorithm [3] make use of either the same ZF filter $\mathbf{G}_V^{(\text{ZF})}$ or the MMSE filter $\mathbf{G}_V^{(\text{MMSE})}$. These filters are the unbiased and biased pseudo-inverses of \mathbf{H}_V , respectively. Since \mathbf{H}_V is a ‘‘tall’’ or ‘‘slim’’ matrix with dimension $M_r \times (M_t - 2)$, computing the ZF or the MMSE filter is significantly simpler than it is with the ACAV channel matrix $\tilde{\mathbf{H}}$ of dimension $2M_r \times 2(M_t - 1)$ as described in [9]. In the pursuit of computational simplicity, the Greville algorithm [12] and the Sherman-Morrison algorithm [13] are adopted to compute $\mathbf{G}_V^{(\text{ZF})}$ and $\mathbf{G}_V^{(\text{MMSE})}$, respectively. In this way, we can evaluate the exact computation required for the GL and GO algorithms.

1) *ZF Detectors for 3×3 ACAV*: The V-symbols from the first and the second time slots in block k , i.e., $a_3(k)$ and $a_4(k)$, are detected as follows:

$$\mathbf{G}_V^{(\text{ZF})} \triangleq \mathbf{g}_3 = \mathbf{h}_3^\dagger = \frac{\mathbf{h}_3^H}{\|\mathbf{h}_3\|^2} \quad (14)$$

$$\hat{a}_3(k) = \mathbb{Q}(\mathbf{g}_3 \mathbf{t}_1(k)), \quad \hat{a}_4^*(k) = \mathbb{Q}(\mathbf{g}_3 \mathbf{t}_2(k)) \quad (15)$$

where \dagger denotes the Moore-Penrose pseudo-inverse operator.

2) *ZF Detectors for 4×4 ACAV*: The pseudo-inverse of $\mathbf{H}_V = [\mathbf{h}_3 \ \mathbf{h}_4]$ can be computed using the Greville algorithm [12] as follows:

$$\mathbf{G}_V^{(\text{ZF})} \triangleq \mathbf{H}_V^\dagger = \begin{bmatrix} \mathbf{g}_3 \\ \mathbf{g}_4 \end{bmatrix} = \begin{bmatrix} \mathbf{h}_3^\dagger - d(\mathbf{h}_4 - d\mathbf{h}_3)^\dagger \\ (\mathbf{h}_4 - d\mathbf{h}_3)^\dagger \end{bmatrix} \quad (16)$$

where $d = \mathbf{h}_3^\dagger \mathbf{h}_4$ and d is a scalar. The linear detector decodes the V-symbols as follows:

$$\begin{aligned} \hat{a}_3(k) &= \mathbb{Q}(\mathbf{g}_3 \mathbf{t}_1(k)), & \hat{a}_4(k) &= \mathbb{Q}(\mathbf{g}_4 \mathbf{t}_1(k)) \\ \hat{a}_5^*(k) &= \mathbb{Q}(\mathbf{g}_3 \mathbf{t}_2(k)), & \hat{a}_6^*(k) &= \mathbb{Q}(\mathbf{g}_4 \mathbf{t}_2(k)). \end{aligned} \quad (17)$$

The OSIC detector extracts the V-symbols in sequential steps as follows. Assuming $\|\mathbf{g}_3\|^2 < \|\mathbf{g}_4\|^2$, then

$$\hat{a}_3(k) = \mathbb{Q}(\mathbf{g}_3 \mathbf{t}_1(k)) \quad (18)$$

$$\mathbf{u}_1(k) = \mathbf{t}_1(k) - \hat{a}_3(k) \mathbf{h}_3 \quad (19)$$

$$\hat{a}_4(k) = \mathbb{Q}(\mathbf{h}_4^\dagger \mathbf{u}_1(k)). \quad (20)$$

If, on the other hand, the SNR is stronger at the 4th channel, i.e., $\|\mathbf{g}_4\|^2 < \|\mathbf{g}_3\|^2$, then

$$\hat{a}_4(k) = \mathbb{Q}(\mathbf{g}_4 \mathbf{t}_1(k)) \quad (21)$$

$$\mathbf{u}_1(k) = \mathbf{t}_1(k) - \hat{a}_4(k) \mathbf{h}_4 \quad (22)$$

$$\hat{a}_3(k) = \mathbb{Q}(\mathbf{h}_3^\dagger \mathbf{u}_1(k)). \quad (23)$$

Independent of the first time slot, $\hat{a}_5^*(k)$ and $\hat{a}_6^*(k)$ of the second time slot are obtained in the same fashion as (18)–(23) above.

3) *MMSE Detectors for 3×3 ACAV*: The MMSE filter of \mathbf{H}_V is

$$\mathbf{G}_V^{(\text{MMSE})} \triangleq \mathbf{g}_3 = \frac{\mathbf{h}_3^H}{\|\mathbf{h}_3\|^2 + \alpha} \quad (24)$$

where α is the ‘‘regularization’’ constant chosen as the ratio of the noise variance to the signal power (of individual transmit antenna) [13]. Subsequently, $\hat{a}_3(k)$ and $\hat{a}_4^*(k)$ are detected in the same manner as (15).

4) *MMSE Detectors for 4×4 ACAV*: The Sherman-Morrison recursion algorithm [13] is used to compute the MMSE filter

$$\begin{aligned} \mathbf{G}_V^{(\text{MMSE})} &\triangleq \begin{bmatrix} \mathbf{g}_3 \\ \mathbf{g}_4 \end{bmatrix} = \mathbf{H}_V^H [\mathbf{H}_V^H \mathbf{H}_V + \alpha \mathbf{I}_{2 \times 2}]^{-1} \\ &= \mathbf{H}_V^H \mathbf{Q}, \end{aligned} \quad (25)$$

where $\mathbf{I}_{2 \times 2}$ is the 2×2 square identity matrix. The Sherman-Morrison algorithm computes \mathbf{Q} in a simple, recursive manner. It starts from the zero-th iteration:

$$\mathbf{Q}_{[0]} = (1/\alpha) \mathbf{I}_{2 \times 2} \quad (26)$$

and then computes the recursion from $n = 1$ to $n = M_r = 4$:

$$\mathbf{Q}_{[n]} = \mathbf{Q}_{[n-1]} - \frac{\mathbf{Q}_{[n-1]} \mathbf{H}_{V,n} (\mathbf{H}_{V,n})^H \mathbf{Q}_{[n-1]}}{1 + (\mathbf{H}_{V,n})^H \mathbf{Q}_{[n-1]} \mathbf{H}_{V,n}} \quad (27)$$

where $\mathbf{H}_{V,n}$ is the n -th column of the ‘‘tall’’ matrix \mathbf{H}_V . The V-symbols are detected in the same manner as (17) for linear detection and (18)–(20) for OSIC with the exception of the pseudo-inverses in (20) and (23) are replaced with the MMSE filter computed in the same fashion as (24).

Table IV
COMPLEXITY ANALYSIS FOR 4×4 RATE-3 MIMO DETECTORS

Detector ($N \times M$)	ZF		MMSE	
	/Frame (Pre-processing) (M, \mathbf{A})	/6-Symbols (Payload) (M, \mathbf{A})	/Frame (Pre-processing) (M, \mathbf{A})	/6-Symbols (Payload) (M, \mathbf{A})
Lin(8×6)	(672, 593.5)	(48, 42)	(840, 606)	(48, 42)
OSIC(8×6)	(792, 705.5)	(48, 80)	(955, 649)	(229, 202)
PWO(8×6)	(716, 639)	(48, 80)	(859, 578)	(229, 202)
GL(4×4)	(32, 17.5)	(56, 46)	(76, 55.5)	(56, 46)
GO(4×4)	(36, 19)	(56, 54)	(80, 46.5)	(56, 54)
V-L(4×3)	(72, 54.5)	(24, 18)	(90, 79.5)	(24, 18)
V-O(4×3)	(98, 76)	(24, 34)	(106, 92.5)	(58, 58)

V. RESULTS

We shall assume the Rayleigh fading channel is stationary over N_{fr} space-time block samples, or equivalently, $2N_{\text{fr}}$ symbol periods.

A. Complexity Analysis

All detectors under consideration achieve the same data throughput, i.e., 3 spatial substreams, and they all have equal number of received antennas, i.e., $M_r = 4$. The ACAV detectors under consideration include the linear detector (Lin), OSIC, pair-wise OSIC (PWO), Group-Linear (GL), and Group-OSIC (GO). The detectors for pure V-BLAST signals are the linear and OSIC detectors, denoted as V-L and V-O, respectively. The dimensions of the channel matrices that the detectors deal with are appended to the names of the detectors, as shown in Table IV, where M and N correspond to the number of effective transmit and received symbols, respectively. We consider both ZF and MMSE implementations of the detectors, and separated the pre-processing (e.g., computing the pseudoinverse of the channel matrix in (16) and (25)) from the payload processing (e.g., linear convolution of equalizer weights and received signal vector in (18) and the subsequent nulling and canceling operations in (19)). The effective channel matrices that need to be pseudoinversed have dimensions 8×6 , 4×2 , and 4×3 for the single-stage, dual-stage, and V-BLAST(4×3) detectors, respectively. After consulting with [12] and [13], we arrived at the following number of pre-processing operations required for the *initialization*, i.e., pseudoinverse of channel matrix, and the *recursion*, i.e., pseudoinverses of subsequent deflated channel matrices, and the number of repetitive payload operations required for every space-time block of N received symbols to compute the linear convolution (e.g., (17), (18)) and the nulling operations (e.g., (19)). For a channel with M and N effective transmit and received symbols, respectively,

1) the Greville-Inverse-Greville algorithm [12]

requires $(\frac{5}{2}M^2N - \frac{1}{2}MN - 3N)\mathbf{M} + (\frac{5}{2}M^2N - M^2 - \frac{3}{2}MN - \frac{5}{2}N + \frac{3}{2})\mathbf{A}$ operations for the “initialization”, while requiring $(\frac{1}{4}M^2N + \frac{1}{4}MN - \frac{1}{2}N)\mathbf{M} + (\frac{1}{4}M^2N - \frac{1}{4}M^2 + \frac{1}{4}MN - \frac{1}{4}M -$

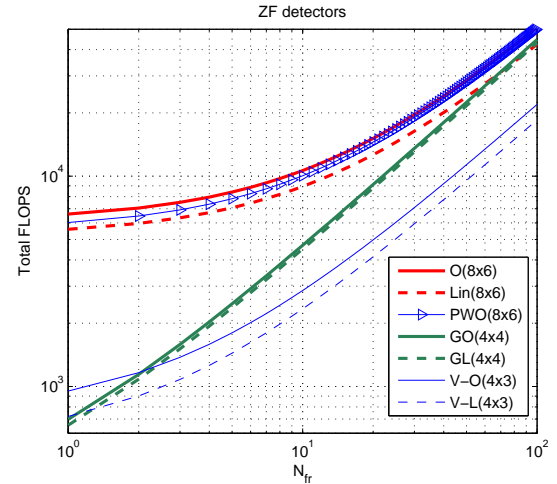


Figure 1. Complexity profile of various detectors with varying N_{fr} . Total FLOPS = FLOPS/frame + N_{fr} *FLOPS/6-symbols.

$\frac{1}{2}N + \frac{1}{2})\mathbf{A}$ for the “recursion”. The computations required for payload processing for a block of N received samples is $(MN)\mathbf{M} + (MN - M)\mathbf{A}$ for the linear detector and $(2MN - N)\mathbf{M} + (2MN - M - N)\mathbf{A}$ for the OSIC detector.

2) the Sherman-Morrison algorithm [13]

requires $(\frac{5}{2}M^2N + \frac{5}{2}MN)\mathbf{M} + (2M^2N - \frac{1}{2}M^2 + MN)\mathbf{A}$ operations for the “initialization”, and $(\frac{2}{3}M^3 - \frac{2}{3}M)\mathbf{M} + (\frac{1}{2}M^3 - \frac{1}{2}M^2 + M + 1)\mathbf{A}$ for the “recursion”. The computation required for every N received data sample is $(MN)\mathbf{M} + (MN - M)\mathbf{A}$ for the linear detector and $(\frac{1}{2}M^2N + \frac{1}{2}M^2 - \frac{1}{2}MN - \frac{1}{2}M)\mathbf{M} + (\frac{1}{2}M^2N - \frac{1}{2}MN - M + 1)\mathbf{A}$ for the OSIC detector.

The PWO requires less complexity than the original OSIC(8×6). More significantly, the PWO detects 6 symbols in 3 sequential IC stages instead of 6, thus the detection speed is doubled. The GL and GO detectors require the least pre-processing and are ideal for rapidly varying channels.

We now investigate the effect of increasing N_{fr} on the complexity of the detector. Each complex multiplication \mathbf{M} requires 6 floating point operations (FLOPs); each complex addition \mathbf{A} requires 2 FLOPs. Although counting FLOPs is not the ideal way to determine the complexity of a detector, it does provide a certain degree of appreciation of the complexity. We compute the total FLOPs by summing the FLOPs per frame and the FLOPs per 6-symbols multiplied by N_{fr} . For small frame sizes, the dual-stage detectors are about 10 times simpler than the traditional ACAV detectors, making them very attractive.

B. Simulation Results

The six detectors are put to test (NB: the performance of OSIC(8×6) and PWO(8×6) are identical). For simplicity,

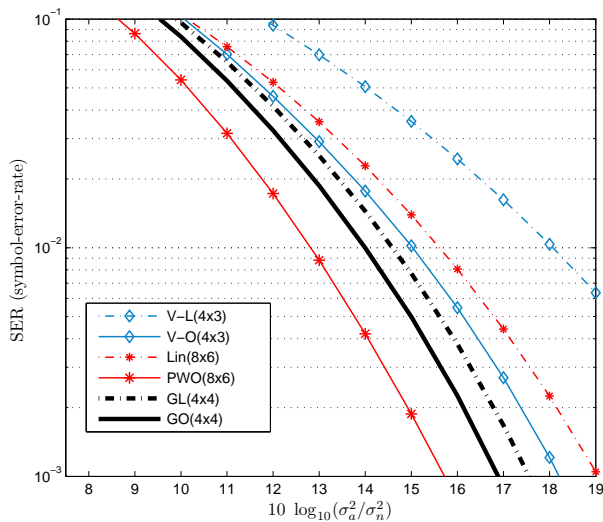


Figure 2. Simulation results comparing the ZF ACAV detectors and V-BLAST 4×3 detectors.

all detectors employ the ZF approach. The modulation scheme is 16-QAM and for each simulation point, 10 million symbols over 100 different random Rayleigh faded channel realizations were used. The result is plotted in Fig. 2.

It is clear that without STBC, the V-BLAST detectors perform poorly against the ACAV detectors. Only the linear ACAV detector performs about 0.5dB worse than the V-O.

As for ACAV detectors, PWO performs the best. The second best is the GO detector with a 1dB gap with the PWO. Following closely to the GO is the GL detector. Interestingly, even the GL performs better than V-O, suggesting the advantage of using the ACAV transmission scheme.

VI. CONCLUSION AND FUTURE WORK

The ACAV has been adopted by IEEE 802.11n-2009 as viable candidates of its hybrid MIMO transmission schemes [5]. Through our simulations we discovered the superiority of ACAV over pure V-BLAST schemes of identical data rate even though similar OSIC or linear detectors were used. That means the ACAV outperforms the V-BLAST as a transmission scheme, and not because of the detector used. In the future, we intend to prove that the ACAV is naturally more resilient to system errors than pure V-BLAST, and perhaps double-space-time-transmit-diversity (D-STTD) [14] too, when the same data rate is enforced. If this is true, the ACAV could replace pure V-BLAST schemes in future broadband modems (WiFi, WiMAX, LTE). Unfortunately the ACAV detectors are relatively complex, so we developed two simple detection schemes in this paper to address this issue.

REFERENCES

- [1] S. Alamouti, "A simple transmit diversity technique for wireless communications," *Selected Areas in Communications, IEEE Journal on*, vol. 16, no. 8, pp. 1451–1458, 1998.
- [2] V. Tarokh, H. JafarKhani, and A. Calderbank, "Space-time block codes from orthogonal designs," *IEEE Trans. Information Theory*, vol. 45, pp. 1456–1467, Jul 1999.
- [3] P. Wolniansky, G. Foschini, G. Golden, and R. Valenzuela, "V-BLAST: an architecture for realizing very high data rates over the rich-scattering wireless channel," *Signals, Systems, and Electronics, 1998. ISSSE 98. 1998 URSI International Symposium on*, pp. 295–300, 1998.
- [4] W. da C. Freitas Jr., F. R. P. Cavalcanti, and R. R. Lopes, "Hybrid transceiver schemes for spatial multiplexing and diversity in MIMO systems," *Journal of Communication and Information System*, vol. 20, no. 3, pp. 63–76, 2005.
- [5] *IEEE Std 802.11n-2009*, (Last assessed 22 Feb 2011).
- [6] *IEEE Std 802.16-2009*, (Last assessed 22 Feb 2011).
- [7] L. Zhang, S. Li, H. Zheng, and M. Wu, "Alamouti code assisted V-BLAST (ACAV): A new space-time architecture," *Communication Technology, 2006. ICCT '06. International Conference on*, pp. 1–4, 2006.
- [8] *IEEE Std 802.16e-2005*, (Last assessed 22 Feb 2011).
- [9] M. Do, W. Chin, and Y. Wu, "Performance study of a hybrid space time block coded system," *Wireless Pervasive Computing, 2006 1st International Symposium on*, 2006.
- [10] L. Zhao and V. K. Dubey, "Transmit diversity and combining scheme for spatial multiplexing over correlated channels," *IEEE 59th Proc. Veh. Technol. Conf.*, vol. 1, pp. 380–383, Spring 2004.
- [11] —, "Detection schemes for space-time block code and spatial multiplexing combined system," *Communications Letters, IEEE*, vol. 9, no. 1, pp. 49–51, Jan 2005.
- [12] Z. Luo, M. Zhao, S. Liu, and Y. Liu, "Greville-to-Inverse-Greville algorithm for V-BLAST systems," *Communications, 2006. ICC '06. IEEE International Conference on*, pp. 4214–4218, 2006.
- [13] J. Benesty, Y. A. Huang, and J. Chen, "A fast recursive algorithm for optimum sequential signal detection in a BLAST system," *IEEE Trans. Signal Processing*, vol. 51, no. 7, pp. 1722–1730, Jul 2003.
- [14] S. Shim, K. Kim, and C. Lee, "An efficient antenna shuffling scheme for a DSTTD system," *IEEE Commun. Letters*, vol. 9, no. 2, pp. 124–126, Feb 2005.